IMPLEMENTATION OF SOLAR PV BASED MICROCONVERTER WITH OPTIMAL MPPT CONTROL UNDER PARTIAL SHADING CONDITION

[1]M.Premkumar, [2]T.R.Sumithira, [3]R.Sowmya

[1]Department of Electrical and Electronics Engineering, KPR Institute of Engineering and Technology, India
[2]Department of Electrical and Electronics Engineering, Government College of Engineering, India
[3]Department of Power Engineering, GMR Institute of Technology, India

[1]mprem.me@gmail.com, [2]sumithira.trs@gmail.com, [3]sowmyanitt@gmail.com

Abstract *— The centralized traditional power grid leads to national power blackout resulting increase in research for alternate solutions. The solar photovoltaic is connected with module integrated converter (MIC) is the efficient way of increasing the performance in now-a-days. The modelling and analysis of such a microconverter with various Maximum Power Point Tracking (MPPT) techniques is simulated with dynamic simulation software in this work. The MPPT algorithm is applied on the SEPIC converter to extract the maximum and optimal power from the panel. The objective of the proposed research is to convert the raw solar energy from the PV cell and supplied to the load with high efficiency and high power quality. The converter includes low voltage stress on the semiconductor devices and simplicity of design. The switching losses are also reduced by replacing with single MOSFET in SEPIC converter. Hence the triggering components and commutation components are reduced while using a MOSFET and therefore the conduction losses are reduced. The converter is analysed with different modern MPPT techniques and this paper concludes optimal MPPT for the converter to extract the maximum power. Finally, the converter is designed for the rating of 80W and optimal MPPT is experimentally verified on the converter.*

Index Terms *— Solar PV, SEPIC converter, Optimal MPPT, Voltage stress, Conduction loss.*

1. Introduction

Module integrated converter are rapidly growing part of the photovoltaic (PV) system. The microinverters are modelled to convert the DC of one PV module to the AC and are designed to get maximum output power in the range of 100W to 300W. The microinverters has advantage in ease of installation, maximum power point tracking (localized), and robustness to failure when compared to conventional string or central inverters shown in fig.1. Since the researchers of power electronics is seeking rapid innovation, there are many different topologies and variations being developed day by day [1]-[2].

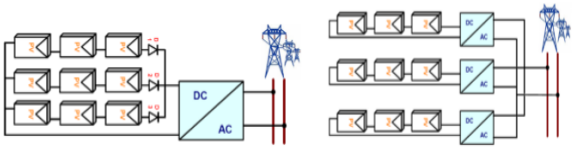


Fig. 1. Central and string topology

Even the string inverter can give more efficiency in capturing energy, the energy obtained from the panel decreases if one of the series PV cell is kept out by shadow as shown in fig. 2.

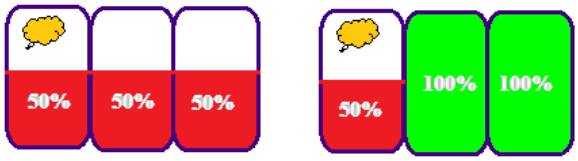


Fig. 2. Energy harvesting

The MIC prefers “distributed MPPT” architecture which adds more cost per PV panel but efficiency is increased by 4 to 20 percent by recovering the following losses:

- PV panel mismatch losses (3.5 to 6 percent)
- Partial shading losses (5 to 25 percent)
- Simpler system design and fault tolerance (0 to 10 percent)
- Suboptimal MPPT losses (3 to 10 percent)

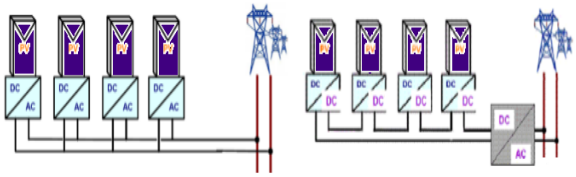


Fig. 3. Basic module integrated converter topology

So, the micro inverters topology as shown in fig.3 which sacrifices the converter efficiency but make the energy capture more efficiently. The microinverter outputs are connected in parallel and routed to a common ac coupling point. To keep dc wiring at relatively low voltage level of a single panel, no series or parallel dc connections are provided [3]-[4].

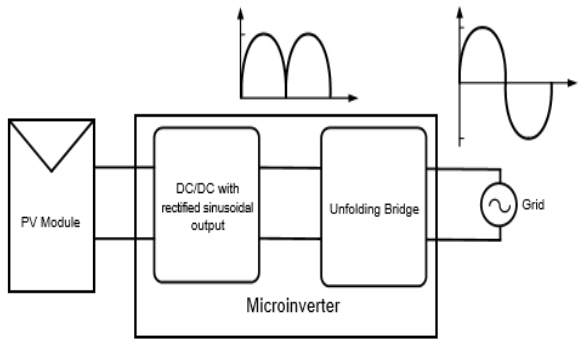
Basically optimal application for specific inverter can be determined from the comparison of the key parameters which is listed in table 1.

BUPT

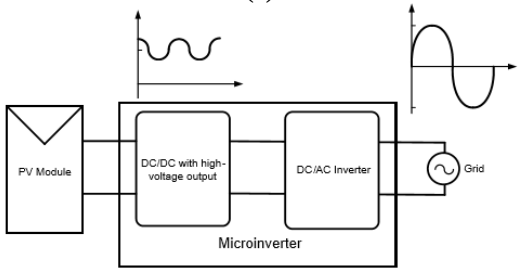
Table I. Key Parameters Comparison of Different Size Inverters

	Nominal Power	Nominal Voltage	Maximum Efficiency	Cost	Cost/ Watt
Microconverter with Inverter	< 300W	< 100V	97.5%	Low	High
String Inverter	< 30kW	150V – 1000V	98%	Medium	Medium
Central Inverter	> 30kW	450V – 1500V	98.5%	Very High	Low

The single-phase microinverter architectures have been reviewed in [5] and the topologies are grouped into single-stage architectures and multistage architectures in fig. 4. In a single stage architecture, voltage and power modulation, and output current shaping are realized in a single power stage but they have low circuit complexity and simple control. Over a wide operating range, it is not possible to achieve high performance. In multistage topology, multiple power conversion stages and each stage can perform one or more functions. The optimization is done individually at each stage, thus the overall performance is better but component requirement and control complexities are usually higher.



(a)



(b)

Fig. 4. (a) Microinverter using a single-stage topology, (b) multi-stage topology

In addition, distributed MPPT terminal for segmented PV arrays can be achieved by single ended primary inductance converter (SEPIC) [6]. There are many configuration for converter such as Buck, Boost, Buck-Boost, SEPIC, CUK and Fly-back and Buck and Boost configurations can decrease and increase the output voltages respectively and others can do both functions [7]. The SEPIC converter must be operated at high switching frequency. However, high switching frequency on the device will increase the reverse recovery current of the output diode which delivers additional switching losses. The high switching frequency will also increase in electromagnetic interference (EMI) noises and additional thermal management. Also, the switch utilization factor of the SEPIC converter is lower than buck-boost converter i.e. the power-handling capabilities of MOSFET in the SEPIC converter are much lower than buck or the boost converter at the same power level. Thus, the reduction of reverse recovery loss is particularly important for the SEPIC converter [9].

MPPT algorithm is important to increase the efficiency of PV module and maintain the PV panel operating point at maximum power point in different irradiance conditions during all day long. The partial shading on the PV panel will reduce the efficiency, increase in complexity and cost. During uniform irradiance, panel exhibits one maximum power point which can be tracked by using conventional MPPT techniques [7]-[8]. But irradiance will not be constant throughout the day and during partial shading, the conventional MPPT will find multiple maximum point due to the bypass diode to prevent hotspot formation on the PV panel. To overcome this problem, many optimized MPPT algorithms are proposed in [13]. Many authors have discussed on the conventional MPPT algorithms for uniform and non-uniform irradiance but the recent advancements in MPPT for solar PV is not being analysed and discussed on SEPIC converter till date. This paper will discuss the adoption of new optimized MPPT for the conventional converter under partial shading condition. The organization of the article is as follows. Section 2 will discuss the PV characteristics on different irradiance condition under partial shading. Section 3 focuses on circuit topology and optimized MPPT techniques for the SEPIC converter. Section 4 deals with modelling, design of SEPIC converter and parameter selection for simulation. Section 5 discusses the hardware and software results of converter with modern MPPT techniques.

The length of the manuscript should be 4–8 pages. If your paper is longer than 8 pages (9 and more), please contact us before uploading it in the interface. At least 75% of the last page should be occupied by text.

All subsequent versions should be uploaded by using the same paper ID and your defined user name and password. We are unable to process files sent by E-mail.

BUPT

2. PV Characteristics under Partial Shading

Change in irradiation and temperature will affect the output of PV panel. When insolation on the PV string is uniform, the power-voltage (PV) curve will show only one peak. But due to partial shading on the panel will show the multiple peak on PV curve which will be having one global maximum power point (GMPP) and many local maximum power points (LMPP).

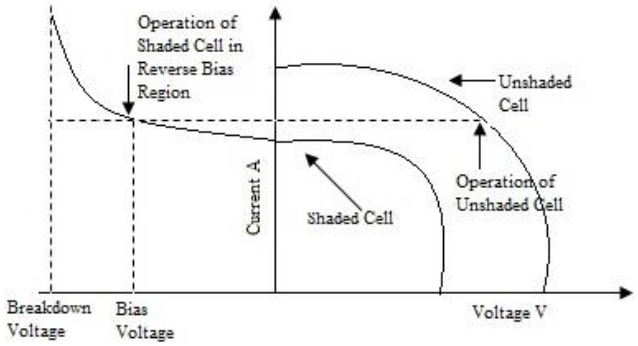


Fig. 5. V-I characteristic of PV cell

Selection of correct GMPP from many LMPP is difficult because a piece of the PV array is able to receive uniform irradiance at partial shading and operates at the optimal efficiency. The shaded PV cells are operated at reverse biased voltage in order to circulate the same current as the unshaded cells since the cells are connected in series. The insolation on PV is directly proportional to short circuit current of PV cell. The operation of shaded cell in reverse biased voltage region for providing the same current is shown in fig. 5.

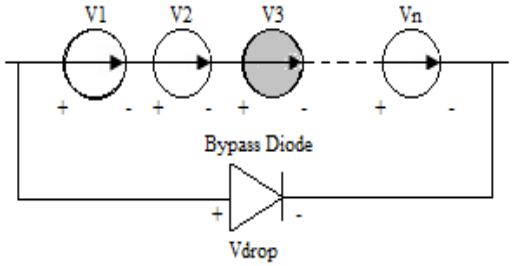


Fig. 6. Operation of bypass diode when cell is shaded

The conduction of the bypass diode during shading condition will takes place when Eq. (1) is satisfied and it is shown in fig. 6.

$$V_2 - \sum_{i=1}^{n} V_i \geq V_{DO}, i \neq 2 \quad (1)$$

Where V_2 is shaded cell voltage and V_{DO} is the voltage drop of the diode.

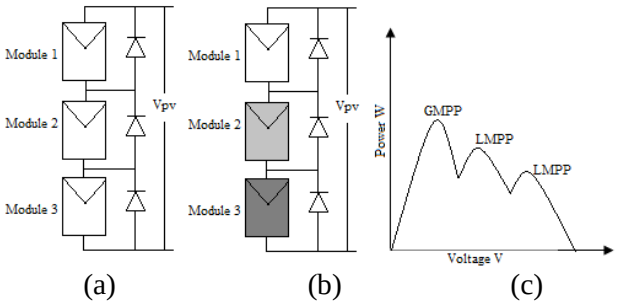


Fig. 7. PV modules (a) Constant irradiance (b) non uniform irradiance (c) Peaks of PV

During partial shading on PV array, the alternate path is provided for the flow of current using bypass diodes as shown in fig. 7(b). The PV characteristic in fig. 7(c) shows many maxima during partial shading condition. The conventional MPPT fails to differentiate LMPP and GMPP, many modern MPPT optimization algorithms are developed and it will be discussed in following section.

3. Circuit Topology

The power stage elements of the proposed converter are as follows. The PV supplies a DC input of 24 V to the dc – dc converter. The SEPIC converter which gives higher or lower output voltage than the given input voltage with the help of MOSFET and energy storage elements. There are two operating modes of the converter depends on the load current flow which may be of Continuous Conduction Mode (CCM) or Discontinuous Conduction Mode (DCM). The SEPIC converter is selected based on its buck-boost capability without inversion of voltage. The storage capacitor is connected across the output and also it serves the supply the difference between the power of the PV panel and double line frequency power variation of the inverter.

3.1 Continuous vs. Discontinuous Conduction Mode

The model simulation and key assumptions are documented in further section. The proposed design has small inductor current ripple in case of CCM as well as large inductor current ripple in case of DCM. The operation of the converter in CCM was suitable for the proposed model because of the ripple in the inductor current is lower and the input current is continuous. Also CCM offers higher efficiency than DCM and voltage gain is independent of the type of load whereas in DCM, voltage gain of the system is depends on the load and designed parameters such as L and switching frequency. But CCM has small switching loss produced by diode reverse recovery. Even though the size of the inductor can be reduced than CCM, the input current is pulsating. The converter can be operated in both modes by defining the power load and the input voltage but the converter in this work is tested in CCM.

BUPT

3.2 MPPT Controller Modelling

Due to the continuous change in insolation and temperature, the current-voltage (I-V) and the power-voltage (P-V) characteristics of a PV module is affected. On both I-V characteristic and P-V characteristics, knee point is defined at which the module can deliver maximum power with maximum efficiency. This knee point is called the maximum power point (MPP) of the PV module. At any environmental condition, the MPP is tracked at the module operates at its maximum efficiency. The control algorithms which tracks the MPP is implemented in conjunction with a power conditioning unit between the PV module and the electrical load.

The implementation of MPP tracking algorithm uses PV module maximum operating voltage, maximum current or power as the input variable and the algorithm generates the reference output which can be used as a control variable which helps to change the duty cycle of the proposed converter. There are many conventional MPP tracking algorithms are exist but in this paper, modern MPP tracking algorithms are discussed which includes:

1) Grey Wolf Optimization (GWO) Technique
2) Artificial Bee Colony (ABC) Optimization
3) Hybrid GWO and Perturb & Observe (P&O)
4) Optimal P&O method
5) Ant Colony Optimization (ACO) and etc.

3.2.1 Grey wolf optimization

The GWO is a heuristic design approach inspired by optimization of attacking techniques of grey wolves proposed in [12]. In order to simulate the hierarchical leadership, they are four various type of grey wolves- omega (ω), delta (δ), beta (β), and alpha (α). The assumption for fittest solution is α. Then, second and third fittest solution is β and δ, ω is represented as the candidate solutions. The hunting, tracking and chasing are the three steps in GWO by forming group, encircling the target and attacking the target. The whole mechanism/process is implemented for optimizing MPPT for PV module. The hunting is guided by the leader α and followed by β. The wounded wolves will be taken care by δ and ω. To keep constant duty cycle and to reduce steady state oscillation, the GWO is combined with the direct duty cycle control (DCC). GWO algorithm flowchart is shown in fig. 8.

The hunting mechanism of grey wolves is modelled according to the following equations:

$$\vec{E} = \left|\vec{C}.\overrightarrow{X_p}(t) - \overrightarrow{X_p}(t)\right| \quad (2)$$

$$\vec{X}(t+1) = \overrightarrow{X_p}(t) - \vec{F}.\vec{E} \quad (3)$$

Where t represents the current iteration, the coefficient vectors are represented by E, F and C, hunting prey is represented by the position vector X_p, and X represents the grey wolf position vector. The coefficient vector F and C are computed as represented in Eq. (4)-(5).

$$\vec{F} = 2\vec{a}.\overrightarrow{r_1} - \vec{a} \quad (4)$$

$$\vec{C} = 2\overrightarrow{r_2} \quad (5)$$

Where a decreases from 2 to 0 linearly and the values $\overrightarrow{r_1}$ and $\overrightarrow{r_2}$ vector in [0,1].

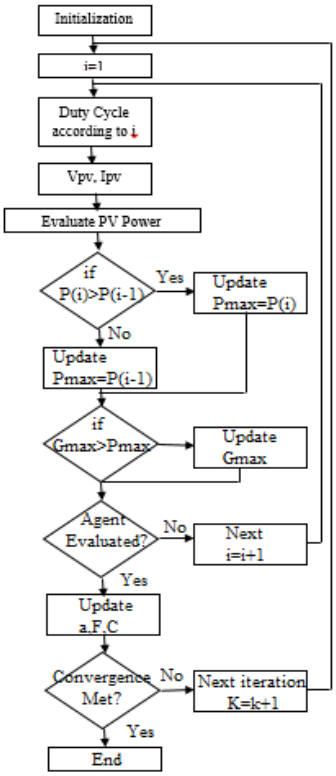


Fig. 8. Grey wolf optimization algorithm flow chart

To reduce oscillation during steady state and power loss in conventional MPPT algorithm, the duty cycle is fixed and normalized. The duty cycle is considered as grey wolf to implement the GWO MPPT. So that, Eq. (3) is modified as Eq. (6) and Eq. (7) gives the GWO fitness function.

$$d_i(k+1) = d_i(k) - F.E \quad (6)$$

$$P(d_i{}^k) > P(d_i{}^{k-1}) \quad (7)$$

Where i is number of current individual grey wolves P is power, d is duty cycle, iteration count is represented by k. GWO technique offers high tracking efficiency with less steady state and transient oscillations.

3.2.2 Artificial bee colony based algorithm

ABC algorithm is a bio-inspired method which is having less controlled parameters, simple, and independent of initial condition. This heuristic

BUPT

algorithm is capable of solving multimodal optimization easily [11]. This algorithm having three important groups such as employed bees, scouts and onlooker bees. The employed bee will search the food or exploits the source of food production, a bee who is waiting in hive and decides the proper selection of the food source is called as onlooker bee and a bee who will be carrying random search for a new food source is called scout bee. The three bees will work, communicating and coordinating together to get the optimal solution in less time. The position of the food is expressed as duty cycle and the food source of ABC algorithm is expressed as maximum power. The flowchart for ABC optimization algorithm as shown in fig. 9 and algorithm is divided into four different phases.

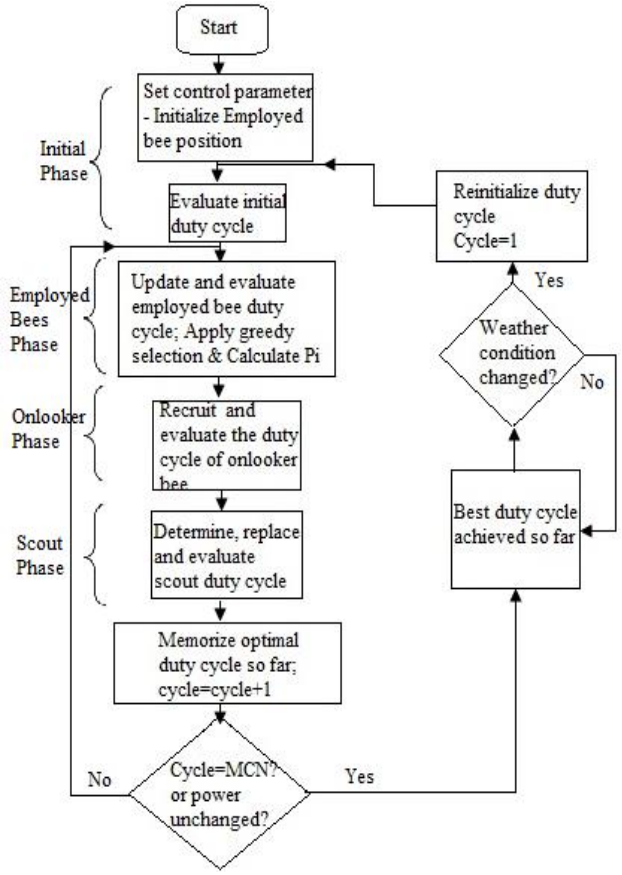


Fig. 9. Flowchart of artificial bee colony optimization

The ABC algorithm is employed for PV system to extract the MPP and the duty cycle for SEPIC converter is calculated as follows:

$$d_c = d_{min} + rand[0,1](d_{max} - d_{min}) \quad (8)$$

$$newd_c = d_c + \varphi_e(d_c - d_p) \quad (9)$$

Where d_c is current duty cycle, d_p is previous duty cycle, d_{min} is minimum value of duty cycle, d_{max} is maximum value of duty cycle, and φ_e is a constant between $[-1,1]$. The ABC algorithm will track MPP with high efficiency and good accuracy under partial shading on PV module.

3.2.3 Hybrid GWO and P&O MPPT algorithm

The hybrid MPPT combines GWO with P&O to extract MPP from the PV module very effectively and efficiently under partial shading condition [13]. The GWO technique as discussed in section 3.2.1 has been combined with the conventional P&O algorithm but the initial phase of MPP is taken care by GWO and P&O is operated for getting GMPP at faster rate. This hybrid algorithm reduces the computational burden and tracks MPP easily. In this MPPT algorithm, the duty cycle for the SEPIC converter is denoted by the position of wolves and it eliminates the use of PI controller in MPPT implementation. The major advantage is that it has fast convergence rate, high speed tracking, and higher efficiency. The fig. 10 shows the hybrid GWO and P&O algorithm flowchart.

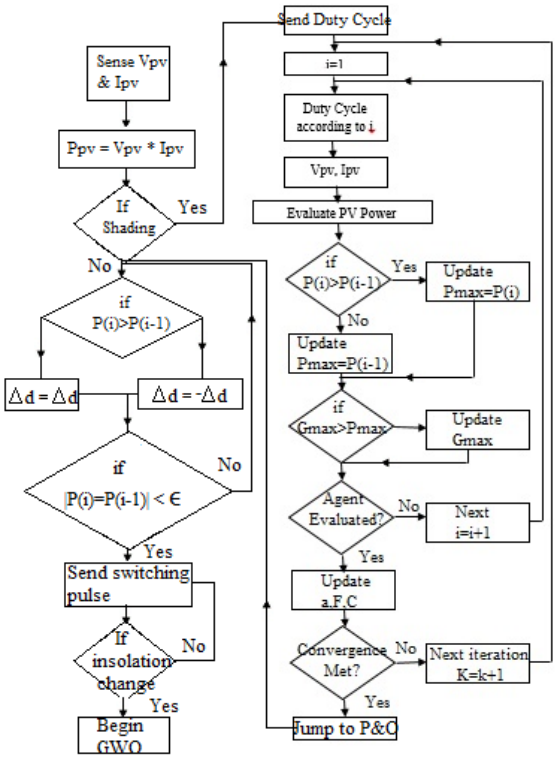


Fig. 10. Flowchart of hybrid GWO and P&O algorithm

4. System Analysis

4.1 Modelling of SEPIC Converter

The SEPIC converter is connected with solar PV module to perform the following major functions:

1) Boost the lower PV voltage
2) Regulate the varying dc output voltage
3) Implement the MPP tracking of the solar panels

The SEPIC converter is selected because of its buck-boost operation without inverting the output voltage. The Eq. (10)-(20) are used to model and design the converter which operates in continuous current conduction mode. The output voltage is given by,

BUPT

$$Vout = Vin * \frac{D}{1-D} \quad (10)$$

Where D is duty cycle of the switching device which is given by,

$$D = \frac{Vout + Vd}{Vout + Vin + Vd} \quad (11)$$

Vd is the forward voltage drop across D_1 and the maximum duty is given by,

$$Dmax = \frac{Vout + Vd}{Vout + Vin(min) + Vd} \quad (12)$$

The inductance value is determined by allowing the peak-peak ripple current to be approximately 40% of the rated input current at the minimum input voltage. The ripple current (ΔIL) flows through the two equal value of inductors which is given by,

$$\Delta IL = Iin * 40\% = Iout * \frac{Vout}{Vin(min)} * 40\% \quad (13)$$

And the two equal inductor values are determined by,

$$L1 = L2 = L = \frac{Vin(min)}{\Delta IL * Fs} * Dmax \quad (14)$$

The peak value of the inductor current which ensures the saturation of the inductor is given by,

$$\Delta IL1(peak) = Iout * \frac{Vout + Vd}{Vin(min)} * \left(\frac{1 + 40\%}{2}\right) \quad (15)$$

$$\Delta IL2(peak) = Iout * \left(\frac{1 + 40\%}{2}\right) \quad (16)$$

The selection of the coupling capacitor (Cs) depends on the RMS current which is given by,

$$Ics(rms) = Iout * \sqrt{\frac{Vout + Vd}{Vin\ (min)}} \quad (17)$$

The SEPIC capacitor is rated for a large RMS current which makes the converter much better for lower power applications where the RMS current through the capacitor is relatively small. The voltage rating of the coupling capacitor is greater than the maximum input voltage. The electrolytic capacitors work well for the proposed work where the size is not limited. The voltage across the coupling capacitor is given by,

$$\Delta Vcs = \frac{Iout * \mathrm{Dmax}}{Cs * Fs} \quad (18)$$

And the coupling capacitor is given by,

$$Cs = \frac{D}{R * \frac{\Delta Vcs}{Vout} * Fs} \quad (19)$$

When the power switch Q1 is turned on, the inductor is charging and the output current is supplied to the load by the output capacitor. As a result, the output capacitor is subjected to large ripple current so that the selected output capacitor must withstand the maximum RMS current. The output capacitor must meet out the require RMS current, equivalent series resistor (ESR) and capacitance requirements. The value of the output capacitor (Co) is given by,

$$Co \geq \frac{Iout * Dmax}{Vripple * Fs} \quad (20)$$

where F_s is the switching frequency; ΔI_{L1} and ΔI_{L2} is peak-to-peak ripple current of inductor L_1 and L_2 respectively; V_{out} is the output voltage; V_{in} is the input voltage from the solar PV module; R is the load resistance. The following tables gives the rating of the PV panel and SEPIC converter.

Table II. PV Panel Specification

Specifications @ G =1000W/m^2 and T=45ºC	
Rated Power (P_{max})	80W
Voltage at P_{max}(V_{mpp})	19.8V
Current at P_{max} (I_{mpp})	4.06A
Short circuit current (I_{sc})	4.8A
Open circuit voltage (V_{oc})	24.4V

Table III. SEPIC Converter Specification

Parameters	**Design Value**
Input voltage range Vin	20-60V
Switching frequency F_s	100kHz
Output voltage V_{out}	400V
Rated output power P_{max}	80W
Current ripple I_{L1}	40%
Input inductor L_1 and L_2	22uH
Coupling capacitor C_s	10uF
Output capacitor C_o	100uF

4.1.1 Operation of the Proposed Converter

Fig. 11 shows a simple schematic diagram of a SEPIC converter which consists of an input capacitor (C_{in}), output capacitor (C_{out}), coupled inductors L_1 and L_2, the coupling capacitor C_s which is charged initially to the input voltage (V_{in}).

BUPT

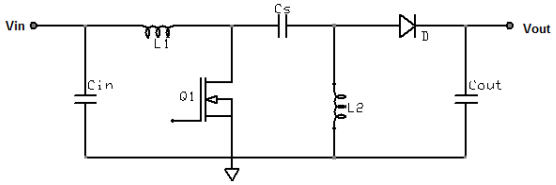


Fig. 11. Proposed SEPIC converter

The converter is operated in CCM if the current through the inductor L_1 will not reaches zero. During the steady state of the converter, the average voltage across the coupling capacitor is equal to the input voltage because the capacitor blocks the DC current so that the average current is zero which makes the inductor L_2 as the source for the load current. Due to V_{L1}=-V_{L2}, the two inductors are wound on the same core. Since the magnitude of the voltage is same, the effect of mutual inductance is zero. And ripple current from two inductors are same in magnitude. So, the current through the inductor L_2 is same as that of load current and it is independent of the input voltage. The input voltage is expressed in Eq. (21),

$$V_{in} = V_{L1} + V_{L2} + V_{cs} \quad (21)$$

As shown in fig. 12, when Q1 is off, the voltage across L_2 must be equal to the output voltage since the input capacitor C_{in} is charged to the input voltage V_{in}. So that the voltage across Q1 when Q1 is off is equal to V_{in} +V_{out} and the voltage across L_1 is equal to the output voltage.

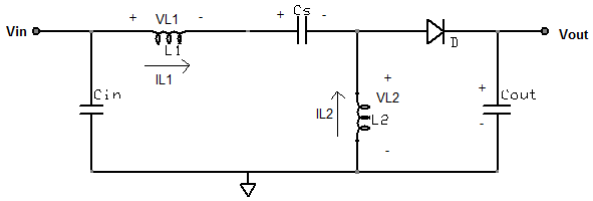


Fig. 12. Q1 in OFF state

As shown in fig. 13, when Q1 is on, the capacitor C_s is charged to V_{in} and it is connected in parallel with L_2, so that the voltage across L_2 is inverse of the input voltage $-V_{in}$. During Q1 on, the currents flowing through circuit elements are shown in fig. 14. When Q1 is on, the energy is stored in L_1 from the input voltage and in L_2 from the coupling capacitor C_s. The average current on the diode D_1 is given in Eq. (22),

$$I_{D1} = I_{L1} - I_{L2} \quad (22)$$

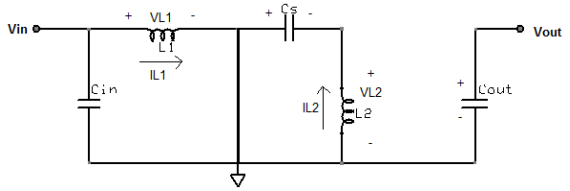


Fig. 13. Q1 in ON state

When Q1 turns off after certain time period, L_1 current continues to flow through C_s and D_1 and finally into the output capacitor C_o and the load. Both the capacitors get recharged so that the capacitors can deliver the load current and charge the inductor L_2, respectively, when Q1 turns on again.

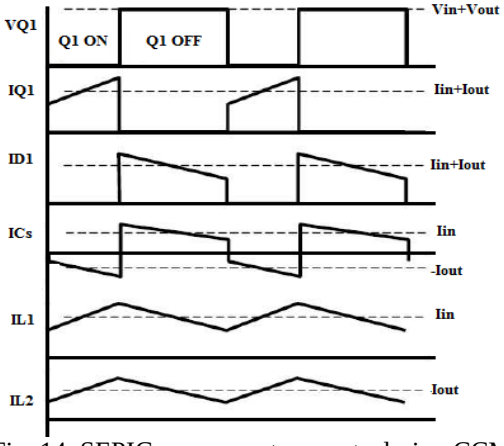


Fig. 14. SEPIC component currents during CCM

4.2 MATLAB/SIMULINK Simulation of SEPIC Converter

The simulation of the SEPIC converter is done with the help of Matlab/Simulink. The parameters are selected as per the table 4. With the below designed parameters, the Simulink model is derived and simulated. The outline of the Simulink model with GWO optimization algorithm is shown in fig. 15.

Table IV. Parameters for MATLAB Simulation

Specifications @ G =1500W/m^2	
Parameters	**Design Value**
PV Panel Voltage	22.6 V
Panel Voltage @P_{max}	20.82
Switching frequency F_s	500kHz
Converter Output voltage V_{out}	167V
Rated output power P_{max}	79.63W
Input inductor L_1 and L_2	22uH
Input Capacitor	4.7uF
Coupling capacitor C_s	7uF
Output capacitor C_o	100uF

The gate signal for the MOSFET is generated by employing modern MPPT optimization techniques which is mathematically modelled in Matlab/Simulink. The mathematical model and its relevant embedded function of the algorithm is shown in fig. 16.

BUPT

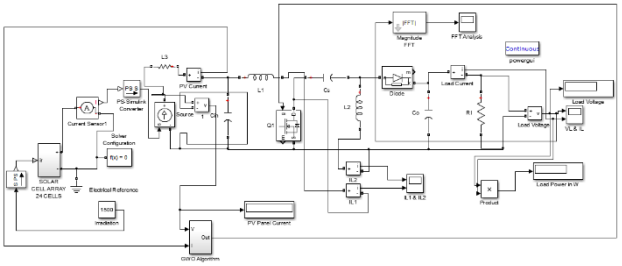


Fig. 15. MATLAB/SIMULINK model of the converter

First, mathematical model of the GWO algorithm is done in the subsystem by receiving the panel voltage and current. The embedded function which serves constant output pulses for the MOSFET for efficient operation and delivers the maximum power with less switching loss.

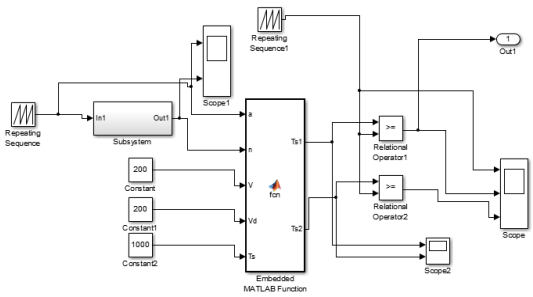


Fig. 16. MPPT simulink model

According to the converter parameters including inductors L_1 and L_2, output capacitor, coupling capacitor, input capacitor, input voltage, output voltage, switching frequency, the converter is operated at CCM since the load is a constant load and the primary inductor current will not reach zero. The output voltage and current is regulated without using PI controllers in the inner control loop.

5. Results and Discussion

The simulation model has been developed for 24 cell PV array, SEPIC converter, MPPT with incremental conductance algorithm using Matlab/Simulink dynamic simulation software. The simulation is done using the designed parameters which is listed in table 4 in section III. The module is designed with PV arrays and string of four modules are connected in series.

5.1 Effect of Changing Temperature on PV Module

The temperature effect on PV voltage for the various solar irradiation and PV characteristics for different irradiation at constant temperature are shown in fig. 17-18. From fig. 17, it is seen that with increase in ambient temperature, the load current of the module is increased, while the open circuit voltage is decreased. The net output power is reduced because of reduction in open circuit voltage with increasing temperature is seen in fig. 18. The effect of changing irradiation on system performance is also shown in fig. 17-18; where it is seen that because of the increase in load current with increase in irradiation which will increase the PV output power.

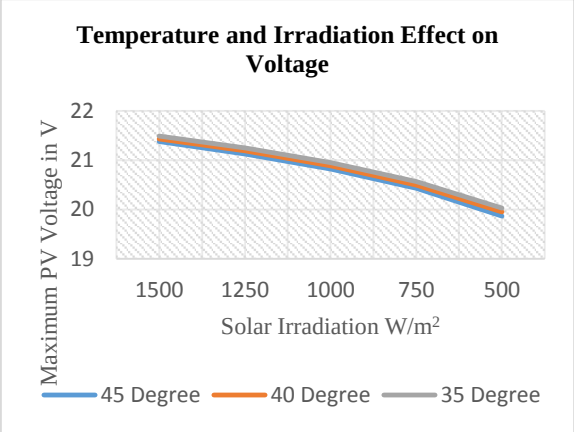


Fig. 17. Temperature effect on PV voltage

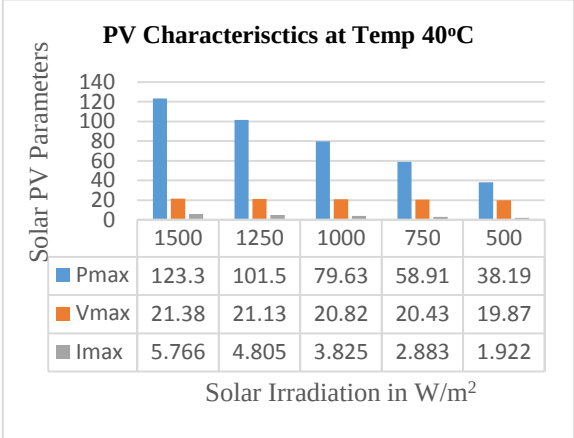


Fig. 18. PV characteristics at temperature 40°C

5.2 Matlab/Simulink Simulation

The model is designed and simulated with Matlab/Simulink dynamic simulation software with the already designed variables as shown in table 4 in section 5. The SEPIC converter load voltage and load current with GWO algorithm is shown in fig. 19. The converter takes finite time to reach the steady state output voltage as shown in fig. 19.

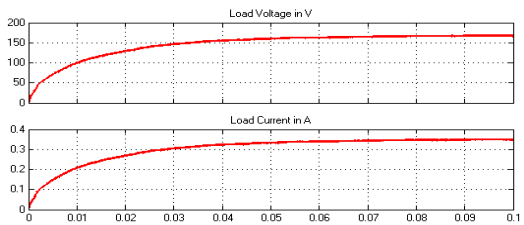


Fig. 19. Converter load voltage and load current

The dynamics of the PV panel and converter under variable insolation and constant load is shown in fig. 20 and fig. 21 respectively is verified by changing the solar

BUPT

irradiation from 750W/m^2 to 900W/m^2 at step time of 2 seconds and then to 1000W/m^2 at 3 seconds.

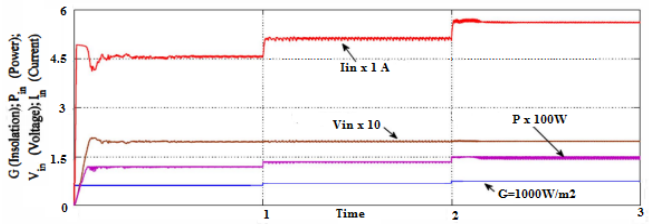


Fig. 20. Dynamics of PV panel under MPPT with insolation variation

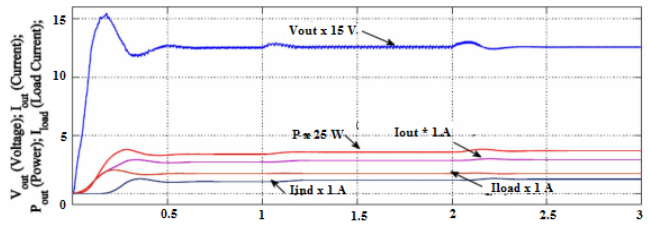


Fig. 21. Dynamics of converter under insolation variation

Before designing pulse width modulation (PWM) switching pulse, the allowed inductor ripple current, ΔI_L need to be decided. If the allowable current is too high, which will increase the electromagnetic interference or if it is too low, results unstable PWM operation. Normally, it is advisable to select 20 to 40% of the input current as the inductor ripple current as computed in [10].

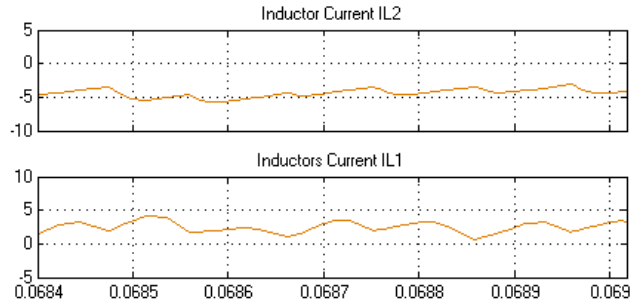


Fig. 22. Inductor currents I_{L1} and I_{L2} at 40% of input current

This work has simulated with the inductor ripple current as 40% of the input current. The inductor currents I_{L1} and I_{L2} is shown in fig. 22.

5.3 Hardware Implementation

The parameters are designed as per the specific input voltage and listed in table 5. The following are the basic data's for deriving the values of other parameters with the assumption of V_d = 0.5V, Rated Power = 80W, Output voltage (V_{out}): 125V, Output current (I_{out}): 1.7A, Switching frequency F_s: 10 kHz.

Table V. Hardware Design Parameters for the Rated Power of 80W

S.No	Parameter Computation	Designed Value	Selected Value
1.	$Dmax = \frac{Vout + Vd}{Vin(min) + Vout + Vd}$ $Dmin = \frac{Vout + Vd}{Vout + Vin(max) + Vd}$	D_{max} = 91.2% D_{min} = 82.4%	D_{max} = 92% D_{min}=82%
2.	The input inductor L_1 ripple, $\Delta IL = Iin * 40\% = Iout * \frac{Vout}{Vin(min)} * 40\%$ So the inductance for L1 and L2 is: $L1 = L2 = L = \frac{Vin(min)}{\Delta IL * Fs} * Dmax$ $\Delta IL1(peak) = Iout * \frac{Vout + Vd}{Vin(min)} * \left(1 + \frac{40\%}{2}\right)$ $\Delta IL2(peak) = Iout * \left(1 + \frac{40\%}{2}\right)$	$\Delta IL = 1.6A$ $L1 = L2 = 22.8\ uH$ $\Delta IL1(peak) = 4.3\ A$ $\Delta IL2(peak) = 0.99\ A$	$L1 = L2 = 22$ uH
3.	The MOSFET peak current, I_{Q1} (peak) = I_{L1} (peak) + I_{L2} (peak) I_{Q1rms}=$Iout\sqrt{\frac{(Vin(min)+Vout+Vd)*(Vout+Vd)}{Vin\ (min)^2}}$ The gate drive current I_g of the IR2110 is 0.3A. The estimated power loss is: P_{Q1} = $I_{Q1\ (rms)}$ * $R_{DS\ (ON)}$ * D_{max} + ($V_{in(min)}$ + V_{out}) * $I_{Q1(peak)}$ * Q_{gd}*F_s / I_g	I_{Q1} (peak) = 5.29 A I_{Q1rms}=4.103A P_{Q1} = 0.92W	MOSFET rated drain voltage must be higher than V_{in}+V_{out}. IRF740n (SiHF740) is selected in this design.

BUPT

4.	SEPIC coupling capacitor selection is: $\Delta Vcs = \frac{Iout * \text{Dmax}}{Cs * Fs}$ $Ics(rms) = Iout * \sqrt{\frac{Vout + Vd}{Vin\ (min)}}$	$\Delta Vcs = 0.452\ V$ $Ics(rms) = 0.935\text{A}$	Ceramic cap is selected with Cs = 10uF
5.	The RMS current of the output capacitor is: $I_{Cout(rms)} = I_{Cs(rms)} = 0.935\text{A}$, $Co \geq \frac{Iout * Dmax}{Vripple * Fs}$	$Co \geq 121uF$	$Co = 100uF$ The electrolytic capacitor is selected due to cost.
6.	Output diode selection is: The reverse rated voltage of the diode should be higher than $V_{in}+V_{out}$ and at full load, the average diode current must be equal to the output current.	-	FR107 is selected because reverse recover voltage as 1000V and average current of 15A

Two inductors are tightly coupled with each having same number of winding on the single core. The mutual inductance between the winding, force the ripple current to split equally between two inductors. But practically, the inductors do not have same inductance so that the ripple current will not be same. In a real coupled inductor, the inductors do not have equal inductance and the ripple currents will not be exactly equal. For the desired ripple current, the inductance is estimated to be half if there are two separate inductors. The experimental setup of the converter is shown in fig. 23 and the converter is tested at 38°C, 1000W/m^2 solar irradiation. The output voltage is obtained from the solar panel under variable conditions. From the observation of variable condition, the voltage from the solar panel is oscillating proportionally.

However, the converter generates an output according to the desired output even though there is a variation in the input voltage. The SEPIC converter is designed to deliver maximum of 80W during partial shading condition. The prototype is tested with three different MPPT optimization technique under partial shading condition.

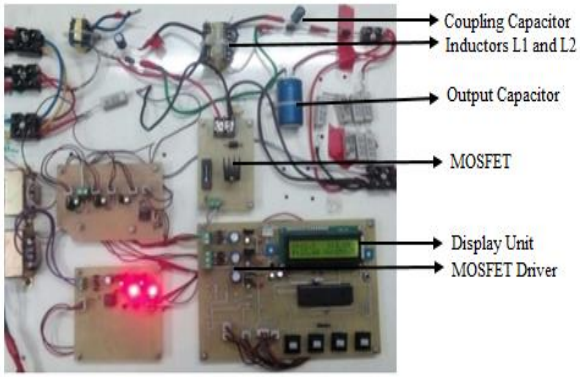


Fig. 23. Converter prototype

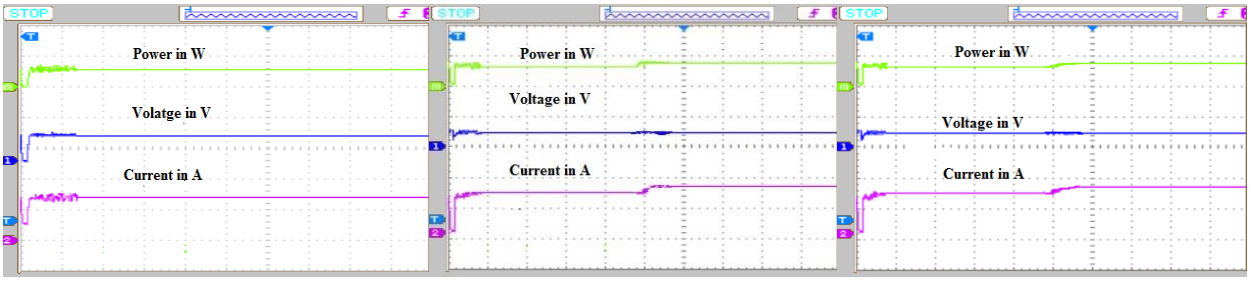
Each optimization technique is having its merits and demerits. The comparison between the optimization techniques are listed in table 6.

Table VI. Summary of Various MPPT Methods

MPPT Technique	Control Strategy	Input Parameters	Output Parameter	Merits	Demerits	Application
GWO	Bio-Inspired	V_{pv}, I_{pv}	Duty Cycle	High efficiency tracking, transient & steady state oscillation is reduced	Computational complexity, high cost	Stand Alone
ABC	Bio-Inspired Evolutionary Algorithm	V_{pv}	Duty Cycle	Simple, fewer control parameters, independent of initial conditions	Tracking is slow, MPP fall on LMPP because of fewer control parameters	Stand Alone
Hybrid GWO and P&O	Bio-Inspired Computational Algorithm	V_{pv}, I_{pv}	Duty Cycle	Tracking performance is superior, oscillation is reduced	Control structure is difficult, high cost, complex	Stand Alone

BUPT

The output voltage and the output current of the converter with GWO algorithm, ABC algorithm and hybrid GWO and P&O is shown in Fig. 24.



(a) (b) (c)

Fig. 24. Voltage (CH1), Current (CH2) and Power of the converter (a) With GWO algorithm; (b) With ABC algorithm; (c) With hybrid GWO and P&O algorithm

From Fig. 24, the convergence time for GWO is 2.9s but for hybrid GWO and P&O is 2.1s. The GWO will track the GMPP at 3.7s without oscillation, ABC will track the GMPP at 4.9s with more oscillation and hybrid tracks the GMPP at 3.5s with less oscillation than ABC algorithm. Thus, the Hybrid GWO and P&O converges faster than other two algorithms but delivers the output with some oscillation. Since, the tracking speed of ABC algorithm much slower than the other two algorithm, it is not preferred for partial shading condition. Since, GWO algorithm offers acceptable convergence rate when compared to ABC algorithm with no steady state and transient oscillation compared to hybrid algorithm, it extract the highest maximum power from the solar PV module with least time. So, it concluded that GWO algorithm can able adopt itself towards variable insolation and partial shading while improves the efficiency of the overall converter. The tracking performance of MPPT is listed in table 7.

Table VII. Tracking Performance Comparison of MPPT Techniques

MPPT	P_{max}	V_{max}	I_{max} in A	Tracking Efficiency
GWO	77.6W	21.32V	3.64A	97%
ABC	76.1W	20.41V	3.72A	95.1%
Hybrid	78.4W	21.30V	3.68A	98%

During different stages, the inductor is charged and charged voltage is supplied to the voltage which is available as SEPIC output. The MOSFET is switched ON and OFF according to the desired output voltage. Charging and discharging of the inductor is shown in fig. 25(a). The voltage across the output capacitor is shown in fig. 25(b).

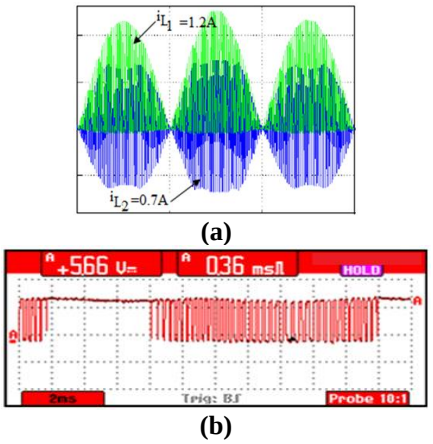


Fig. 25. Various output waveforms (a) Inductor currents I_{L1} & I_{L2}, (b) Output capacitor voltage

The estimated loss of the converter with GWO is shown in table 8. The efficiency of the converter is acceptable and may be suitable for PV based distributed generation station.

Table VIII. Power Loss in Converter with Optimal GWO

Type of the loss	Predicted Loss
Switching loss	1.451
Conduction loss	1.110
Inductor losses	0.621
MOSFET driver power consumption	0.245
Controller power consumption	0.147
Total Loss	3.574
Efficiency at the rated power is 95.53%	

6. Conclusions

In this work, the SEPIC converter modelling in CCM has been done with modern MPPT optimization algorithm. The Matlab/Simulink simulation results indicates that PV electric power production is highly environmental condition dependent and the maximum output power of the solar PV module can be achieved electronically by GWO MPPT algorithm. The two inductors L1 and L2 are wound on the same core so that

BUPT

the same/constant voltages are applied to the inductor throughout the switching period. The switching device current rating will determine and decides the SEPIC converter maximum output current. Since the power rating of the converter is low, the selected switching device SiHF740 MOSFET offers very less conduction loss and switching loss so that it will withstand peak voltage and current of the system. The converter is designed and controlling is implemented with low power and low cost ATMEGA microcontroller which consumes less power and reliability of the converter also appreciable. This papers briefs the modelling and implementation of DC-DC converter topology with modern optimization algorithm being used in module integrated converter today. From the comparison, it was found that GWO will be best suitable and optimal for SEPIC converter than other two algorithms.

In future, the converter control will be implemented with DSP processor or FPGA for high power rating but for the rating below 100W, ATMEGA controller might be suitable.

References

[1] Chen B., Gu B., Zhang L., Z. Ullah Zahid, Jih-Sheng (Jason) Lai, Liao Z., and Hao R.: *High-Efficiency MOSFET Transformerless Inverter for Nonisolated Microinverter Applications*. In: IEEE Transactions on Power Electronics, XXX (2015), No.7, July 2015, p.3610-3622.

[2] Zhang D.: *AN-1484 Designing a SEPIC Converter*. In: Texas Instrument Application Report-SNVA168E, May 2006 and Revised on April 2013, p. 01-11.

[3] Meneses D., Garcıa O., Alou P., Jesus A. Oliver and Jose A. Cobos: *Grid-Connected Forward Microinverter with Primary-Parallel Secondary-Series Transformer*. In: IEEE Transactions on Power Electronics, XXX (2015), No.9, September 2015, p.4819-4830.

[4] Tao J. and Xue V.: *Grid-Connected Micro Solar Inverter Implement Using a C2000 MCU*. In: Texas Instrument Application Report, May 2013, p.01-35.

[5] Chen .M, Khurram K. Afridi and David J. Perreault: *A Multilevel Energy Buffer and Voltage Modulator for Grid-Interfaced Microinverters*. In: IEEE Transactions on Power Electronics, XXX (2015), No.3, March 2015, p.3070-3080.

[6] Ramkumar M., Sayed mohammed I., and Manikanda prashath J.: *Simulation of SEPIC-CHMLI based Microinverter for High Step-up Voltage Conversion*. In: International Journal of Innovative Research in Science, Engineering and Technology, III (2014), No.4, April 2014, p.10871-10880.

[7] Premkumar M., Dhanasekar N., Dhivakar R., and Arunkumar .P: *Comparison of MPPT Algorithms for PV Systems based DC – DC Converter*. In: Advances in Natural and Applied Sciences, XVII (2016), No.9, September 2016, p.212-221.

[8] Premkumar M., Jeevanantham .R, and Muthuvigneshkumar S.: *Single Phase Module Integrated Converter Topology for Microgrid Network*. In: International Journal of Innovative Research in Electrical, Electronics, Instrumentation and Control Engineering, II (2014), No.3, March 2014, p.1322-1325.

[9] Muoka P.I., Haque M.E., Gargoom A., and Negnevitsky M.: *Modeling and Simulation of a SEPIC Converter based Photovoltaic System with Battery Energy Storage*. In: Proc. of 22nd Australian Universities Power Engineering Conference, November 26-29, 2012, Australia, p.01-06.

[10] Eng V., Pinsopon U., and Bunlaksananusorn C.: *Modeling of a SEPIC Converter Operating in Continuus Conduction Mode*. In: Proc. of 6th International Conference on Electrical Engineering / Electronics, Computer, Telecommunications and Information Technology, May 6-9, 2009, Thailand, p.136-139.

[11] Benyoucef A.S., Chouder A., Kara .K, Silvestre .S, and Aitsahed O.: *Artificial bee colony based algorithm for maximum power point tracking (MPPT) for PV systems operating under partial shaded conditions*. In: Applied Soft Computing, XXXII (2015), No.C, July 2015, p. 38-48.

[12] Mohanty S., Subudhi B., and Pravat Kumar Ray: *A New MPPT Design Using Grey Wolf Optimization Technique for Photovoltaic System under Partial Shading Conditions*. In: IEEE Transactions on Sustainable Energy, VII (2016), No.1, January 2016, p.181-188.

[13] Rezaee Jordehi A.: *Maximum power point tracking in photovoltaic (PV) systems: A review of different approaches*. In: Renewable and Sustainable Energy Reviews, LXV (2016), November 2016, p. 1127–1138.